

# A Wind-PV Hybrid Generation Scheme for Grid-Isolated Remote Application



Sarang A. Khadtare, Boni Satya Varun Sai, and Debashis Chatterjee

## 1 Introduction

Nowadays, the world is facing a severe energy crisis due to rapid growth in industrialization as well as in population. The scarcity of fuel, its polluting effects on environment, and continuously increasing prices are some of the actualities related to conventional fuel. Thus, free and large availability of renewable energy sources with non-polluting nature increases the interest of the researchers around the world. There are many generation schemes based on renewable energy sources [1–5]. These schemes are designed either by considering single source such as wind, PV, hydro or with the combination of these for grid-connected or grid-secluded mode [1–4]. The single renewable source-based schemes are easy to design but the reliability of system under the variable environmental conditions is the matter of concern for grid-isolated operation. Hybrid renewable energy generating system has two or more distributed energy sources with or without battery. For the electrification of remote and difficult locality, the hybrid generation system with battery is considered as most potent [3–6]. In last few decades, the wind and PV become very popular among all the other renewable energy sources due to their suitability for ease of conversion [1–3]. For the grid-isolated and grid-connected wind-PV hybrid scheme, the SCIG is very common [2–4]. The SCIG is robust in construction and has a negligible maintenance requirement with excellent controllability; therefore, it is widely preferred for grid-secluded operation at inaccessible locations [4]. The single-phase induction generator supplies the domestic loads [5–8]. In case of SCIG, the value of excitation capacitor affects the output generated voltage. The problem of voltage unbalance arises if the SCIG is provided with fixed reactive power under change in wind velocity and load. Under such circumstances, for maintaining the generated voltage constant, the technique of capacitor switching [9] or auxiliary series-connected capacitor can be used [10]. However, this technique introduces harmonics in output voltage as switching is not

---

S. A. Khadtare (✉) · B. S. V. Sai · D. Chatterjee  
Department of Electrical Engineering, Jadavpur University, Kolkata, India

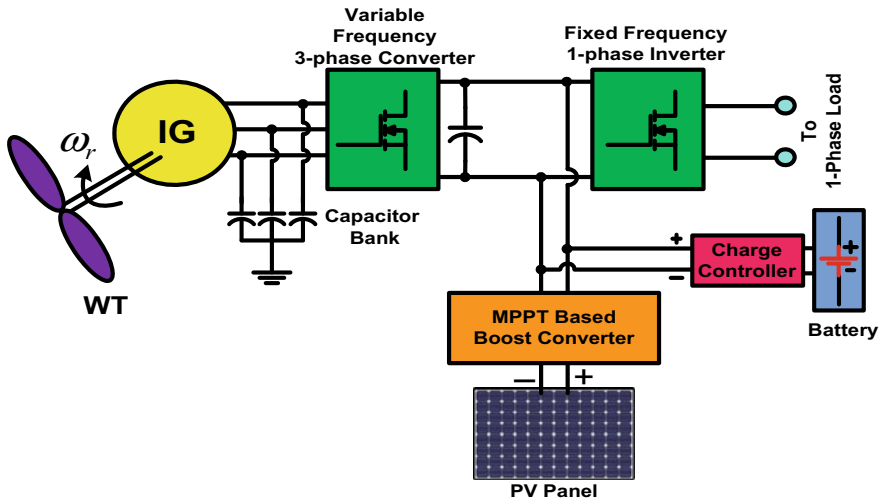


**Fig. 1** Block diagram of proposed generation scheme

smooth. Doubly fed induction generator (DFIG) offers better control and generation capabilities for grid-connected system [11–13]. But this system is affected by several issues like high maintenance, poor reliability (due to the use of mechanical contacts), higher cost, and poor power factor. The various control techniques for asymmetrical operation of three-phase SCIG are presented in [14–19]. Few articles demonstrate the hybrid system with wide wind speed operation of SCIG [14, 20]. The hybrid generation schemes with complex control methodologies, e.g., vector control with loss minimization, dynamic voltage restorer (DVR)-based control, have been demonstrated in [21–24].

Among different hybrid control schemes, the wind-PV-based systems are most popular as these sources are complementary in nature. The major drawback of such system for grid-isolated operation is the optimal battery capacity selection considering low-speed operation. The battery is a component which increases system installation cost as well as maintenance cost which reflects in effective energy pricing.

In this paper, a method has been described to design optimum battery capacity considering grid-secluded operation. The starting condition for the IG with low wind speed and low solar insolation has been considered for optimal battery capacity selection. The proposed method has been tested in a 1 kW hybrid generation system which showed promising results.

## 2 Proposed Generating Scheme

Figure 1 represents the schematic diagram of proposed hybrid generation scheme. It consists of two renewable energy source of wind and PV along with the power

converters and battery. In order to generate the energy from wind, aero turbine coupled with three-phase SCIG is employed. Initially, essential reactive power to the SCIG under no load condition is provided by the stator-connected capacitor bank. These excitation capacitors act as the fixed source of reactive power. Under variable load and wind speed conditions, the variable reactive power is required by SCIG. This necessity is fulfilled by a variable frequency bidirectional converter connected at stator terminals of SCIG. To obtain the maximum energy from the wind, the three-phase bidirectional converter is to be strategically triggered. The triggering pulses of converter are generated corresponding to maximum power points of the turbine characteristics as shown in Fig. 4. The solar panel is connected across the common DC bus. The PV module is interfaced with DC bus through a boost converter, which can also supply power to load during no or low wind condition. In order to obtain the maximum power from PV, the triggering of boost converter is controlled by MPPT controller. The DC power available at common bus is converted into single-phase AC by means of fixed frequency single-phase inverter. This generated AC voltage is applied across the terminals of single-phase domestic loads. The battery is incorporated as a standby storage for reactive power source for the generator during starting or low wind condition. In case of no wind and no PV condition, the battery can also supply critical loads for a limited period of time. The bidirectional DC-DC converter is connected as a charge controller for a battery.

### 3 Proposed Control Strategy

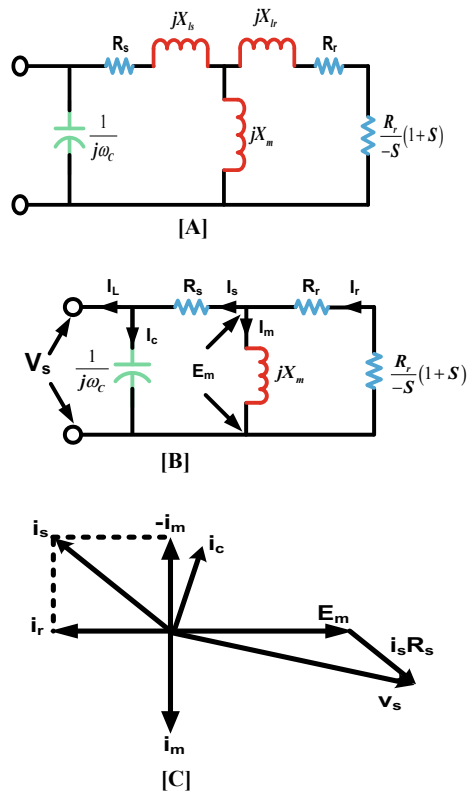
The inverter connected with the SCIG provides variable reactive power at variable frequencies depending on the wind speed. Thus, during starting, as the turbine has low speed, the impressed frequency by inverter to the stator of SCIG is low. The line frequency equivalent circuit for the SCIG has been provided in Fig. 2a. On the other hand, low frequency equivalent circuit for the SCIG is given below in Fig. 2b. In this paper, the battery capacity has been calculated based on the requirement that the battery is only required for maintaining the wind generation during the starting of turbine at low speed when the PV generation is absent of feeble. The battery is not for continuous operation to supply load. This can reduce installation and replacement cost which ultimately results in considerably reduced energy pricing.

The selection of stator side capacitor  $C$  is usually based on no load and rated conditions where it can supply the reactive power required for establishing the machine flux. Thus, at no load the reactive power requirement is mainly for the magnetizing flux. So the values of  $C$  in per phase basis can be approximately given by,

$$C = \frac{1}{\omega_{\text{rated}}^2 L_m} \quad (1)$$

For the proposed method of battery capacity selection, an extreme case is considered where PV power availability is negligible and the wind speed is low. The machine

**Fig. 2** a Equivalent circuit of SCIG b Equivalent circuit of SCIG at low frequency c Phasor diagram under load



is started at no load with low wind speed where the operating slip is also very low. Therefore, at low slip near  $S = 0$  the rotor current  $i_r$  will be negligible. Thus, from equivalent circuit in Fig. 2b, the fixed capacitor current  $i_c$  will be lesser than the magnetizing current  $i_m$ , i.e.,  $i_c < i_m$ . This is because at low speed the generated voltage and frequency will be low as evident from the  $V-f$  plot shown in Fig. 3. The fixed capacitor current  $i_c$  is given by,

$$i_c = v\omega C \tag{2}$$

Or,

$$i_c = \frac{V\omega}{\omega_{rated} 2L_m} \tag{3}$$

Also,

$$V = \frac{V_{rated} \times \omega}{\omega_{rated}} \tag{4}$$

**Fig. 3** Voltage  $V_s$  frequency ( $v-f$ ) plot

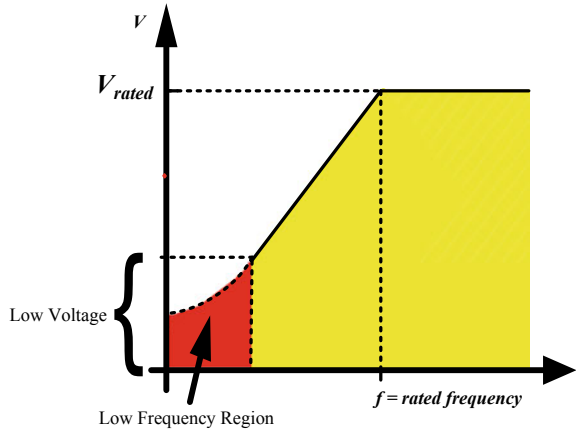
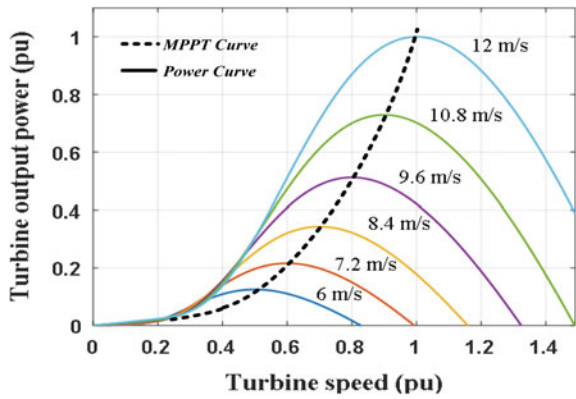


**Fig. 4** Wind turbine characteristics at different wind velocities



Hence, the above Eq. 3 is given by,

$$i_c = \left( \frac{\omega}{\omega_{rated}} \right)^2 \times \left( \frac{V_{rated}}{\omega_{rated} L_m} \right) \tag{5}$$

$$i_c = \left( \frac{\omega}{\omega_{rated}} \right)^2 i_m \tag{6}$$

On the other hand, the magnetizing current  $i_m$  can be expressed as,

$$i_m = \frac{V}{\omega L_m} \tag{7}$$

where  $V$  is the stator side voltage of SCIG and  $\omega$  is the generated angular frequency.

Since  $V$  and  $\omega$  change almost proportionally, the magnetizing current  $i_m$  can remain at rated value whereas at low speed  $\left(\frac{\omega}{\omega_{\text{rated}}}\right)$  value is less giving  $i_c$  to a low value from Eq. 2. Therefore, the balance current  $(-i_c + i_m)$  has to be supplied from the inverter through battery. At any other speed within the operating range, the terminal voltage can be obtained from the  $V$ - $f$  plot as given in Fig. 3. Thus, the approximate battery capacity in VA can be calculated as,

$$VA_{\text{Battery}} = \sqrt{3} V_L i_m \quad (8)$$

Therefore, as observed from Fig. 3 the fixed capacitor current calculated from Eq. 2 will increase with higher frequency which can result in lesser battery current requirement to maintain generator flux. Thus, low-speed situation is the worst condition for battery sizing calculation. The battery rating can be decided by the voltage at IG terminal obtained from Fig. 3 multiplied by current requirement. The amp-hrs. rating of the battery can be decided by the consideration of time for which the low-speed situation can persist. This can be obtained from the meteorological data for the installed region.

The reactive power requirement at low speed during starting when current is  $(i_m - i_c)$  given by,

$$Q = \sqrt{3} V_L (i_m - i_c) \quad (9)$$

From Eq. 1, the value of  $C$  is calculated at no load condition. Thus, the value of  $i_m$  is always the rated value. Under such condition, the capacitor current  $i_c$  is negligibly small, and hence, the reactive power requirement is given by,

$$Q = \sqrt{3} V_L i_m \quad (10)$$

So, battery volt-ampere rating (VA) can be calculated by considering the standard battery rating of 48 V. The battery current rating can also be determined. This low-speed situation will not exist for a long duration as wind flow increases suddenly. Therefore, for analysis purpose we are considering a short duration of 2 h. Thus, the current rating of a battery can be calculated by using Eq. 10 as,

$$\text{Battery current rating} = \frac{\sqrt{3} V_L i_m}{\text{Battery Voltage}} \quad (11)$$

Similarly, the amp-hr capacity of a battery with safety factor of 1.2 can be calculated as for 2 h,

$$\text{Amp-hr Capacity} = \text{Current Capacity of Battery} \times 2 \text{ Amp-hr}$$

On the other hand, the power that can be supplied through stator under this condition is low and can be available from the turbine data. Thus,  $I_r$  can be calculated

**Table 1** SCIG parameters

|                                      |               |
|--------------------------------------|---------------|
| KW                                   | 500 W         |
| Voltage                              | 415 V         |
| Rated speed                          | 1500 rpm      |
| Power factor                         | 0.8 lag       |
| Stator resistance                    | 13.2 $\Omega$ |
| Rotor resistance                     | 19.1 $\Omega$ |
| Magnetising inductance               | 950 mH        |
| Stator and rotor leakage inductances | 85 mH         |

with corresponding slip data. The battery capacity can be effectively calculated and compared with higher speed requirement. For the proposed 1 kW system with SCIG of 500 W and PV system of 500 W, the calculated minimum battery capacity is 50Ah, 12 V. This battery can supply the required magnetizing current for 16 h at no load at wind speed of one-third of the rated value with no PV power generated. Since the wind power generated at lower speed can be also low, the effect of load on this battery size is almost negligible with only reduction of time duration by marginal amount (Fig. 4).

## 4 Simulation Result

The MATLAB–Simulink package is used to simulate the proposed scheme. For simulation purpose a three-phase 500 W, 415 V, 1500 rpm squirrel cage induction machine is used as SCIG. The various parameters of simulated SCIG and wind turbine are given in Table 1. Figure 5a shows the plot for generator speed of value 500 rpm specifying low frequency operation of SCIG. Figure 5b shows the plot for inverter phase voltage having peak value of 108 V. Figure 5c shows the plot for capacitor current having value of 0.25 amp. Figure 5d shows the plot of generator speed of value 800 rpm. Figure 5e shows the plot for inverter generated voltage having peak value of 175 V. Figure 5f shows the plot for capacitor current having value of 0.5 amp at 800 rpm. MATLAB–Simulink model of the proposed scheme is shown in Fig. 6 (Table 2).

## 5 Conclusion

In case of hybrid generation, the battery sizing is one of the important factors along with the various controlling strategies, and it has to be addressed. In this research work, the methodology is proposed for calculating the optimum sizing of the battery considering the worst scenario of low-speed operation with no PV insolation. The

**Fig. 5** Simulation results  
**a** Generator speed 500 rpm.  
**b** Inverter output phase voltage (108 V). **c** Capacitor current (0.25 amp).  
**d** Generator speed 800 rpm.  
**e** Inverter output phase voltage (174 V). **f** Capacitor current (0.5 amp)

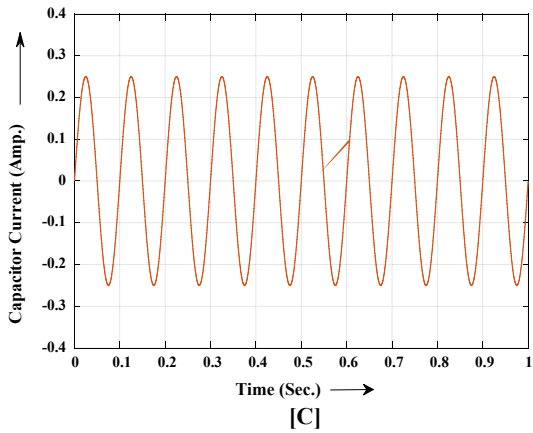
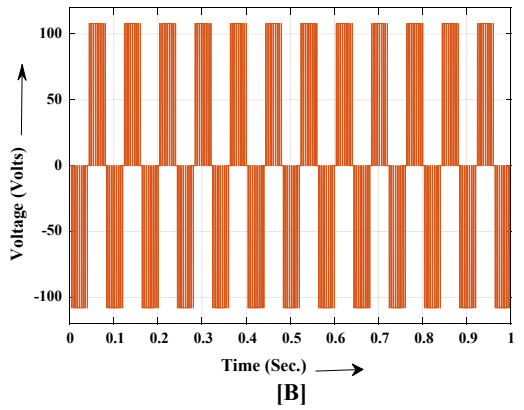
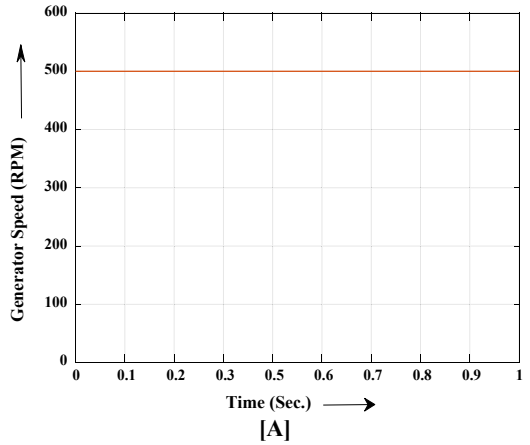
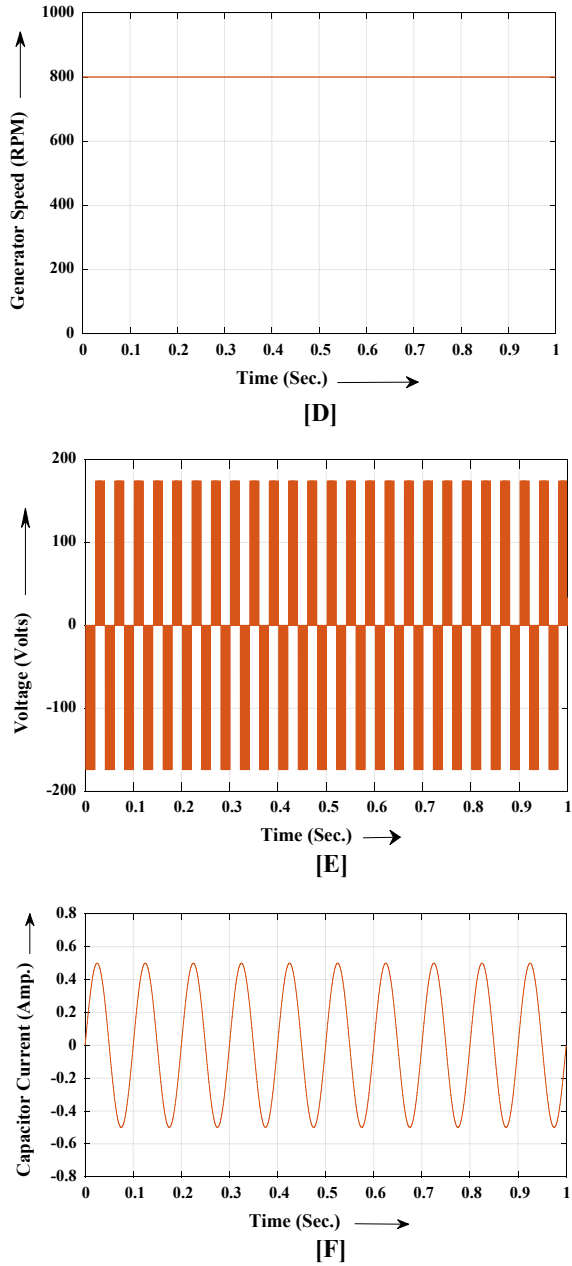




Fig. 5 (continued)





**Table 2** Wind turbine parameters

|                           |         |
|---------------------------|---------|
| Diameter                  | 2.75 m  |
| Optimal tip speed ratio   | 8.5     |
| Optimal power coefficient | 0.41    |
| Power output at 12 m/s    | 2000 W  |
| Cut-in wind speed         | 4.5 m/s |

proposed method for battery sizing has been practically tested to verify simulation results.

**Acknowledgements** The authors acknowledge the Ministry of New and Renewable Energy, India for funding this research work with file no.- 24/22/2016-SWES(R&D).

## References

1. Blaabjerg, F., & Ma, K. (2013). Future on power electronics for wind turbine systems. *IEEE Journal of Emerging and Selected Topics in Power Electronics*, 1(3), 139–152.
2. Patel, M. R. (2006). *Wind and solar power systems: Design, Analysis and Operation*. Boca Raton, FL, USA: CRC Press.
3. Bansal, R. C., Bhatti, T. S., & Kothari, D. P. (2005). A bibliographical survey on induction generators for application of nonconventional energy system. *IEEE Transactions on Energy Conversion*, 18(3), 433–439.
4. Bansal, R. C. (2003). Three-phase self-excited induction generators: An overview. *IEEE Transactions on Energy Conversion*, 20(2), 292–299.
5. Murthy, S. S. (1993). Anovel self-induced self-regulated single phase induction generator. *IEEE Transactions on Energy Conversion*, 8(3), 377–382.
6. Rahim, Y. H. A., Alolah, A. I., & Al Mudaiheem, R. I. (1993). Performance of single phase induction generators. *IEEE Transactions on Energy Conversion*, 8(3), 389–395.
7. Ojo, O., & Bhat, I. (1995). An analysis of single phase self-excited induction generators. *IEEE Transactions on Energy Conversion*, 10(2), 254–260.
8. Ojo, O. (1995). The transient and qualitative performance of a self-excited single-phase induction generator. *IEEE Transactions on Energy Conversion*, 10(3), 493–501.
9. Ahmed, T., Noro, O., Hiraki, E., & Nakaoka, M. (2004). Terminal voltage regulation characteristics by static Var compensator for a three-phase self-excited induction generator. *IEEE Transactions on Industry Application*, 40(4), 978–988.
10. Chauhan, P. J., & Chatterjee, J. K. (2019). A novel speed adaptive stator current compensator for voltage and frequency control of standalone SEIG feeding three-phase four-wire system. *IEEE Transactions on Sustainable Energy*, 10(1), 248–256.
11. Vicatos, M. S., & Teqopoulos, J. A. (1989). Steady state analysis of a doubly-fed induction generator under synchronous operation. *IEEE Transactions on Energy Conversion*, 4(3), 495–501.
12. Xing, X., Meng, H., Xie, L., Yue, L., & Lin, Z. (2019). Switching performance improvement based on model—predictive control for wind turbine covering the whole wind speed range. *IEEE Transactions on Sustainable Energy*, 10(1), 290–300.
13. Xu, H., Hu, J., & He, Y. (2012). Integrated modeling and enhanced control of DFIG under unbalanced and distorted grid voltage conditions. *IEEE Transactions on Energy Conversion*, 27(3), 725–736.

14. Chatterjee, A., & Chatterjee, D. (2019). An improved current balancing technique of two-winding IG suitable for Wind-PV-based grid-isolated hybrid generation system. *IEEE Systems Journal*, 4(4), 4874–4882.
15. Smith, O. J. M. (1987). Three phase induction generator for single phase line. *IEEE Transactions on Energy Conversion*, 2(3), 382–387.
16. Chan, T. F., & Lai, L. L. (2001). Steady-state analysis and performance of stand-alone three-phase induction generator with asymmetrically connected load impedances and excitation capacitances. *IEEE Transactions on Energy Conversion*, 16(4), 327–333.
17. Gao, S., Bhuvaneswari, G., Murthy, S. S., et al. (2014). Efficient voltage regulation scheme for three-phase self-excited induction generator feeding single-phase load in remote locations. *IET Renewable Power Generation*, 8(2), 100–108.
18. Arthishri, K., Kumaresan, N., & Gounden, N. A. (2019). Analysis and application of three phase SEIG with power converters for supplying single phase grid from wind energy. *IEEE System Journal*, 13(2), 1813–1822.
19. Chatterjee, A., & Chatterjee, D. (2016). Analysis and control of photovoltaic assisted three-phase induction machine operating as single-phase micro-wind generator. *IET Generation Transmission and Distribution*, 10(9), 2156–2176.
20. Wandhare, R. G., & Agarwal, V. (2015). Novel integration of a PV-wind energy system with enhanced efficiency. *IEEE Transactions on Power Electronics*, 30(7), 3638–3649.
21. Castillo, J. P., Mafiolis, C. D., Escobar, E. C., Barrientos, A. G., & Segura, R. V. (2015). Design, construction and implementation of a low cost solar-wind hybrid energy system. *IEEE Latin America Transactions*, 13(10), 3304–3309.
22. Leidhold, R., Garcia, G., & Valla, M. I. (2002). Field oriented controlled induction generator with loss minimization. *IEEE Transactions on Industry Electronics*, 49(1), 147–156.
23. Mesemanolis, A., Mademlis, C., & Kioskeridis, I. (2013). Optimal efficiency control strategy in wind energy conversion system with induction generator. *IEEE Journal of Emerging and Selected Topics in Power Electronics*, 1(4), 238–246.
24. Leon, A. E., Farias, M. F., Battaiotto, P. E., et al. (2011). Control strategy of a DVR to improve stability in wind farms using squirrel-cage induction generators. *IEEE Transactions on Power Systems*, 26(3), 1609–1617.